

Generalized Gradient Flows with Provable Fixed-Time Convergence and Fast Evasion of Non-Degenerate Saddle Points

Mayank Baranwal, Param Budhraja, Vishal Raj, and Ashish R. Hota, *Member, IEEE*

Abstract—Gradient-based first-order convex optimization algorithms find widespread applicability in a variety of domains, including machine learning tasks. Motivated by the recent advances in fixed-time stability theory of continuous-time dynamical systems, we introduce a generalized framework for designing accelerated optimization algorithms with strongest convergence guarantees that further extend to a subclass of non-convex functions. In particular, we introduce the *GenFlow* algorithm and its momentum variant that provably converge to the optimal solution of objective functions satisfying the Polyak-Łojasiewicz (PL) inequality, in a fixed-time. Moreover for functions that admit non-degenerate saddle-points, we show that for the proposed GenFlow algorithm, the time required to evade these saddle-points is bounded uniformly for all initial conditions. Finally, for strongly convex-strongly concave minimax problems whose optimal solution is a saddle point, a similar scheme is shown to arrive at the optimal solution again in a fixed-time. The superior convergence properties of our algorithm are validated experimentally on a variety of benchmark datasets.

Index Terms—Accelerated optimization, Fixed-time convergence, Minimax problem, Continuous-time optimization, Saddle point evasion

I. INTRODUCTION AND RELATED WORK

Consider the unconstrained optimization problem

$$\min_{x \in \mathbb{R}^n} f(x), \quad (1)$$

where the function $f : \mathbb{R}^n \rightarrow \mathbb{R}$ is a differentiable function. A large class of algorithms have been proposed to find an optimal solution of the above problem. Due to several computationally attractive properties, the class of gradient-based first-order optimization algorithms have seen wide applicability in machine learning tasks [1], [2]. In order to obtain faster convergence guarantees, accelerated gradient methods have been proposed and analyzed as well [3]–[5].

The above class of algorithms iteratively update the candidate solutions based on (local estimate of) the gradient of the objective function. Thus, the evolution of the candidate solutions assumes the form of a discrete-time difference equation. Convergence of the iterates to the optimal solution are typically analyzed from a discrete-time viewpoint [1], [2].

Mayank Baranwal is with the Tata Consultancy Services Research, Mumbai, Maharashtra 400607, India (e-mail: baranwal.mayank@tcs.com).

Param Budhraja is with the Department of Electrical and Computer Engineering, Boston University, Boston, MA 02215, USA (e-mail: paramb@bu.edu).

Vishal Raj and Ashish R. Hota are with the Department of Electrical Engineering, Indian Institute of Technology, Kharagpur, West Bengal 721302, India (e-mails: vishalrajroy@iitkgp.ac.in, ahota@ee.iitkgp.ac.in).

More recently, inspired by the seminal paper [6], several works have started to view the evolution of the candidate solutions from the lens of a continuous-time dynamical system whose equilibrium point coincides with the optimal solution, and convergence to the equilibrium is tied to its stability property. For instance, the simple gradient descent algorithm for minimizing a convex function f can be mapped to a continuous-time dynamical system using the gradient flow $\dot{x}(t) = -\nabla f(x(t))$.

Analysis of the resulting nonlinear dynamical system not only provides fresh insights into the convergence behavior of the underlying optimization algorithm [6], [7], but it also enables leveraging advanced results from the field of control theory [8], [9] to propose new algorithms with improved stability properties associated with the optimal solution leading to accelerated convergence guarantees and under more general assumptions [10]–[13].

In particular, the notion of finite-time stability [14] was examined in [15] and [12] in the context of continuous-time gradient-flows. In this work, we focus on the recently developed notion of fixed-time stability (FxTS) [16], which strengthens the notion of finite-time stability and provides fastest convergence guarantees. In particular, an equilibrium point is globally fixed-time stable if the dynamics reaches the equilibrium point in a finite amount of time which can be uniformly upper bounded for all initial conditions. Leveraging the above notion of stability, the authors in [13], [17] propose the fixed-time stable gradient flow (FxTS-GF) scheme, given by

$$\dot{x} = -c_1 \frac{\nabla f(x)}{\|\nabla f(x)\|^{\frac{p-2}{p-1}}} - c_2 \frac{\nabla f(x)}{\|\nabla f(x)\|^{\frac{q-2}{q-1}}},$$

with $c_1, c_2 > 0$, $p > 2$, $q \in (1, 2)$ under which the optimizer of f is shown to be a fixed-time stable equilibrium when f satisfies the PL-inequality [18]. In particular, a function $f : \mathbb{R}^n \rightarrow \mathbb{R}$ satisfies PL-inequality with modulus $\mu > 0$ if

$$\frac{1}{2} \|\nabla f(x)\|^2 \geq \mu (f - f^*), \quad (2)$$

where $f^* := f(x^*)$ is the minimum value of the function attained at x^* . Note that all strongly-convex functions satisfy PL-inequality, however, the converse is not true in general. In fact, functions that satisfy the PL-inequality need not be convex. For instance, the cost function in the logistic regression problem over a compact set is not strongly-convex, nevertheless, it satisfies the PL-inequality. In addition, for

functions satisfying PL-inequality, every stationary point is a global minimum.

The above scheme (FxTS-GF) is closely related to the class of first order algorithms with a re-scaled or normalized gradient descent [19]–[21] which have been shown to escape non-degenerate saddle points more efficiently compared to the conventional gradient descent scheme; the latter may take exponentially long to escape certain saddle points.

The algorithms discussed above, namely (stochastic) gradient descent (SGD) [22], rescaled gradient descent [6], [20], [21] and fixed-time stable gradient flow [13] are characterized by constant learning rates across each dimension of the decision variable. As a result, the descent magnitude often gets dominated by the largest absolute component of the gradient vector, leading to larger descent steps in some dimensions and smaller steps in others. This poses a significant challenge in high-dimensional non-convex problems, such as the ones that arise in the context of training neural networks. In contrast, algorithms such as Adam [23] often exhibit improved convergence behavior due to element-wise normalization of the gradient vector resulting in uniform scaling of effective learning rates across each dimension [24], [25].

A. Statement of Contributions

In this work, we propose a novel continuous-time gradient flow, termed *GenFlow*, which includes element-wise normalization to adaptively scale the learning rates for each dimension. It generalizes element-wise scaling algorithms, such as Adam [23], to guarantee (accelerated) fixed-time convergence for a large class of convex as well as non-convex cost functions. We further provide bounds on escape time from non-degenerate saddle points. Our main contributions are summarized below.

- 1) **Fixed-Time and accelerated convergence for a sub-class of non-convex problems:** Most existing accelerated gradient algorithms provide faster convergence guarantees only for a special class of convex functions satisfying strong convexity and/or Lipschitz-smoothness [3], [26]. In contrast, we prove that under the proposed GenFlow scheme and its momentum variant, the optimal solution is fixed-time stable for the class of cost functions satisfying the PL inequality [18], which also includes non-convex cost functions. This is in contrast to [13] where the authors assume strong convexity and Lipschitz-smoothness on the cost function to design a momentum variant of a fixed-time convergent algorithm that is discontinuous and exhibits significant chattering near the optimal solution.

- 2) **Fixed-time evasion of non-degenerate saddle points:**

In high-dimensional non-convex optimization problems, including problems that arise in the context of training neural networks, the proliferation of non-degenerate saddle points induces a significant challenge for optimization algorithms [27]. While the gradient descent algorithm can evade saddle points and converge to the local minima [28], the learning rate could be vanishingly slow and time to escape from the vicinity of a saddle

point can be exponentially large [20], [27], [29]. Recent work has shown both empirically and theoretically that GD with normalization tend to evade saddle points more efficiently [19], [20], [30]. We show that the proposed GenFlow scheme is not only capable of escaping non-degenerate saddle points, but the time of evasion is also uniformly bounded for all initial conditions.

- 3) **Accelerated convergence for min-max problems:** In addition to cost minimization problems, the class of min-max or *saddle point* problems arise in several settings including game theory [31], machine learning [32], [33] and statistics [34]. We extend the proposed GenFlow scheme to this class of problems and show that for a strongly convex-strongly concave objective function, a saddle point can be reached uniformly in a fixed-time.
- 4) **Empirical performance:** The proposed GenFlow algorithm and its momentum variant are used for training neural networks and generative adversarial networks (GANs) and are shown to outperform state-of-the-art (SOTA) algorithms including Adam, root mean squared propagation (RMSProp), stochastic variance reduced gradient (SVRG) and fixed-time stable gradient flow (FxTS-GF).

Notation: The set of all real numbers is denoted \mathbb{R} and the n -dimensional Euclidean space is denoted by \mathbb{R}^n . For a vector $x \in \mathbb{R}^n$ the notation x^\top is used for its transpose. The ℓ_p norm for $p \geq 1$ is denoted by $\|\cdot\|_p$, and when p is not specified $\|\cdot\|$ denotes the ℓ_2 norm. The set of functions $f : U \rightarrow V$, where $U \subseteq \mathbb{R}^n$ and $V \subseteq \mathbb{R}^m$, that are k -times continuously differentiable is denoted by $C^k(U, V)$. For a function $f \in C^1(\mathbb{R}^n, \mathbb{R})$, ∇f denotes its gradient. The i^{th} component of the gradient vector ∇f is denoted by $\nabla_i f$. The Hessian of $f \in C^2(\mathbb{R}^n, \mathbb{R})$ is denoted by $D^2 f$.

The set of all eigenvalues of a matrix $A \in \mathbb{R}^{n \times n}$ is called its spectrum and is denoted by $\sigma(A)$. An eigenvalue $\lambda \in \sigma(A)$ with minimum absolute value is denoted by $|\lambda|_{\min}(A)$, i.e. $|\lambda|_{\min}(A) = \min_{\lambda \in \sigma(A)} |\lambda|$. Similarly $|\lambda|_{\max}(A)$ denotes the eigenvalue with maximum absolute value. The open ball of radius r around $x \in \mathbb{R}^n$ is denoted by $B_r(x) := \{y \in \mathbb{R}^n : \|y - x\|_2 < r\}$. For $n \geq 1$ the n -dimensional Lebesgue measure is denoted by \mathcal{L}^n .

Background and Preliminary Results

Below we present a few preliminary results that enable us to establish fixed-time convergence guarantees. We first formally define fixed-time stability of an equilibrium point and then present a sufficient condition for it.

Definition 1 (Fixed-Time Stability [16]). *Consider the autonomous differential equation:*

$$\dot{x}(t) = g(x(t)), \quad \text{with} \quad g(0) = 0. \quad (3)$$

The origin of (3) is defined to be globally fixed-time stable (FxTS), if it is Lyapunov stable and there exists a uniform settling time $\bar{T} < \infty$, independent of the choice of the initial condition $x(0)$, s.t.,

$$x(t) = 0 \quad \text{for all } t \geq \bar{T} \quad \text{and any } x(0) \in \mathbb{R}^n.$$

Lemma 1 (Fixed-time stability [16]). *Let $V : \mathbb{R}^n \rightarrow \mathbb{R}$, $V \in C^1$ be a continuously differentiable Lyapunov function with $V(0) = 0$ and $V(x) > 0$ for all $x \in \mathbb{R}^n \setminus \{0\}$, and*

$$\dot{V}(x(t)) \leq -aV(x(t))^{\gamma_1} - bV(x(t))^{\gamma_2},$$

with $a, b > 0$, $\gamma_1 \in (0, 1)$ and $\gamma_2 > 1$, then the origin of (3) is globally FxTS with

$$\bar{T} \leq \frac{1}{a(1 - \gamma_1)} + \frac{1}{b(\gamma_2 - 1)}.$$

Remark 1. *Lemma 1 not only provides sufficient condition for existence of a fixed-time stable equilibrium, but also provides an upper-bound on the uniform settling-time \bar{T} in terms of the parameters a, b, γ_1, γ_2 . Thus, given the total budget on solving for the equilibrium point of (3), the parameters can be tuned so that convergence is guaranteed in the prescribed budget.*

Our main convergence theorem relies on the following power inequality lemma which is a direct consequence of the Hölder's inequality [35].

Lemma 2 (Power Inequality). *For a vector $z = (z_1, z_2, \dots, z_n) \in \mathbb{R}^n$, the following holds:*

$$\left| \sum_{i=1}^n z_i \right|^p \leq \begin{cases} \sum_{i=1}^n |z_i|^p, & p \in (0, 1], \\ n^{p-1} \sum_{i=1}^n |z_i|^p, & p > 1. \end{cases} \quad (4)$$

II. FIXED-TIME CONVERGENCE OF GENFLOW

Motivated by the adaptive scaling properties of algorithms with element-wise normalization, and fixed-time stability properties of dynamical systems, we propose the following gradient flow scheme, termed as *GenFlow*, for the problem (1):

$$\dot{x}_i = -\frac{\nabla_i f(x)}{|\nabla_i f(x)|^{\frac{p-2}{p-1}}} - \frac{\nabla_i f(x)}{|\nabla_i f(x)|^{\frac{q-2}{q-1}}} \quad \text{for } i = 1, 2, \dots, n, \quad (5)$$

where $p > 2$ and $q \in (1, 2)$. In practice, the scheme (5) is implemented by adding a small ϵ to the denominators in order to avoid potential divisibility by zero. Unlike the fixed-time convergent flow described in [13], the proposed GenFlow scheme adaptively scales the learning rate for each dimension through an element-wise normalization. We now establish convergence guarantees of GenFlow for optimization of functions that satisfy the PL-inequality (2).

Theorem 1 (GenFlow Fixed-Time Convergence). *Let $f : \mathbb{R}^n \rightarrow \mathbb{R}$ be a continuously differentiable function satisfying PL-inequality. Then the GenFlow scheme defined by (5) converges to the optimal solution of f in a fixed-time independent of the initialization.*

Proof of Theorem 1. We begin by considering the following candidate Lyapunov function:

$$V(x) := f(x) - f^*, \quad (6)$$

where $f^* = \min_{x \in \mathbb{R}^n} f(x)$. Let $x^* = \operatorname{argmin}_{x \in \mathbb{R}^n} f(x)$ and $f(x^*) = f^*$. Notice that the Lyapunov function is positive definite, i.e., $V(x) > 0$ for all $x \neq x^*$. The choice of Lyapunov

function is also motivated by the definition of PL-inequality. Taking the time-derivative of V along the trajectories of (5) yields:

$$\begin{aligned} \dot{V} &= \sum_{i=1}^n \nabla_i f(x) \dot{x}_i \\ &= -\sum_{i=1}^n |\nabla_i f(x)|^{2 \cdot \frac{p}{2(p-1)}} - \sum_{i=1}^n |\nabla_i f(x)|^{2 \cdot \frac{q}{2(q-1)}}, \\ &\leq -\left(\sum_{i=1}^n (\nabla_i f(x))^2 \right)^{\frac{p}{2(p-1)}} - n^{\frac{q-2}{2(q-1)}} \left(\sum_{i=1}^n (\nabla_i f(x))^2 \right)^{\frac{q}{2(q-1)}} \\ &\leq -(2\mu V)^{\frac{p}{2(p-1)}} - n^{\frac{q-2}{2(q-1)}} (2\mu V)^{\frac{q}{2(q-1)}}, \end{aligned}$$

where the second last inequality follows from Lemma 2 and the last inequality follows from the PL-inequality. Observe that for the given choices of p and q , we have $\frac{p}{2(p-1)} < 1$ and $\frac{q}{2(q-1)} > 1$, i.e., the sufficient conditions for fixed-time convergence stated in Lemma 1 are satisfied. Thus the GenFlow scheme guarantees uniform convergence in a fixed time. Recall that the uniform settling time can further be obtained in terms of the parameters μ, n, p and q as stated in Lemma 1. \square

A. Accelerated Convergence via Momentum: GenFlow(M)

Despite adaptive scaling for each dimension, pathological curvature conditions may halt optimizer's progress along certain directions. In such scenarios, optimizers can be further accelerated using momentum-like updates [36]. In light of this, we introduce the momentum variant of the GenFlow which we refer to as GenFlow(M):

$$\begin{aligned} \dot{v}_i &= \nabla_i f(x) - v_i \left(\frac{1}{|v_i|^{\frac{p-2}{p-1}}} + \frac{1}{|v_i|^{\frac{q-2}{q-1}}} \right), \\ \dot{x}_i &= -v_i - \nabla_i f(x) \left(\frac{1}{|\nabla_i f(x)|^{\frac{p-2}{p-1}}} + \frac{1}{|\nabla_i f(x)|^{\frac{q-2}{q-1}}} \right), \\ &\quad \text{for } i = 1, 2, \dots, n, \end{aligned} \quad (7)$$

with $p > 2$ and $q \in (1, 2)$. Below we show that the GenFlow(M) flow converges to the optimal solution uniformly in a fixed amount of time.

Theorem 2 (GenFlow(M) Fixed-Time Convergence). *Let $f : \mathbb{R}^n \rightarrow \mathbb{R}$ be a continuously differentiable function satisfying PL-inequality. Then the GenFlow scheme defined by (7) converges to the optimal solution of f in a fixed-time independent of the initialization.*

Proof of Theorem 2. Note that the equilibrium point of GenFlow(M) (7) is given by the tuple $(x, v) = (x^*, 0)$. Since f satisfies PL-inequality, a natural choice for the candidate Lyapunov function is:

$$V(x, v) := (f - f^*) + \frac{1}{2} \sum_{i=1}^n v_i^2. \quad (8)$$

Taking the time-derivative of V along the trajectories of (7) yields:

$$\begin{aligned}
\dot{V} &= \sum_{i=1}^n \nabla_i f(x) \dot{x}_i + \sum_{i=1}^n v_i \dot{v}_i \\
&= - \sum_{i=1}^n (\nabla_i f(x))^{2 \cdot \frac{p}{2(p-1)}} - \sum_{i=1}^n (\nabla_i f(x))^{2 \cdot \frac{q}{2(q-1)}} \\
&\quad - \sum_{i=1}^n v_i^{2 \cdot \frac{p}{2(p-1)}} - \sum_{i=1}^n v_i^{2 \cdot \frac{q}{2(q-1)}} \\
&\leq - \left(\sum_{i=1}^n (\nabla_i f(x))^2 \right)^\alpha - \left(\sum_{i=1}^n v_i^2 \right)^\alpha \\
&\quad - n^{\frac{q-2}{2(q-1)}} \left(\left(\sum_{i=1}^n (\nabla_i f(x))^2 \right)^\beta + \left(\sum_{i=1}^n v_i^2 \right)^\beta \right), \quad (9)
\end{aligned}$$

where the last inequality follows from Lemma 2 with $\alpha = \frac{p}{2(p-1)}$ and $\beta = \frac{q}{2(q-1)}$. Using the PL-inequality, (9) can further be written as:

$$\begin{aligned}
\dot{V} &\leq - (2\mu(f - f^*))^\alpha - \left(\sum_{i=1}^n v_i^2 \right)^\alpha \\
&\quad - \underbrace{n^{\frac{q-2}{2(q-1)}}}_\kappa \left((2\mu(f - f^*))^\beta - \left(\sum_{i=1}^n v_i^2 \right)^\beta \right) \\
&\leq -2^\alpha \min(1, \mu^\alpha) \left((f - f^*)^\alpha + \left(\frac{1}{2} \sum_{i=1}^n v_i^2 \right)^\alpha \right) \\
&\quad - \kappa 2^\beta \min(1, \mu^\beta) \left((f - f^*)^\beta + \left(\frac{1}{2} \sum_{i=1}^n v_i^2 \right)^\beta \right), \\
&\leq -2^\alpha \min(1, \mu^\alpha) V^\alpha - 2\kappa \min(1, \mu^\beta) V^\beta, \quad (10)
\end{aligned}$$

where the last inequality is again obtained using Lemma 2. Recall that (10) satisfies the sufficient condition for fixed-time stability, thus guaranteeing fixed-time convergence. \square

Remark 2 (Note on algorithmic implementation). *It is important to note that while continuous-time dynamical systems viewpoint enables rigorous convergence analysis of an optimization algorithm, in practice, it is inevitable to use a discrete-time, iterative method to solve optimization problems. While we consider simple Euler-discretization of GenFlow in our experiments, GenFlow(M) is discretized using step-sizes (β, η) as follows:*

$$\begin{aligned}
v_i(k+1) &\approx \beta \left(\frac{v_i(k)}{|v_i(k)|^{\frac{p-2}{p-1}}} + \frac{v_i(k)}{|v_i(k)|^{\frac{q-2}{q-1}}} \right) + (1-\beta) \nabla_i f(x(k)), \\
x_i(k+1) &= x_i(k) - \eta \left(v_i(k+1) + \frac{\nabla_i f(x(k))}{|\nabla_i f(x(k))|^{\frac{p-2}{p-1}}} \right. \\
&\quad \left. + \frac{\nabla_i f(x(k))}{|\nabla_i f(x(k))|^{\frac{q-2}{q-1}}} \right).
\end{aligned}$$

Here $\beta \in (0, 1)$ can be understood as the momentum parameter, while η represents the learning rate.

III. SADDLE POINT EVASION IN A FIXED TIME

As discussed earlier, classical gradient descent algorithm often slows down in the neighborhood of a saddle point as the gradient has small magnitude in this neighborhood. In this section, we show that due to the normalization term $|\nabla_i f(x)|^{-\frac{p-2}{p-1}}$, the magnitude of the vector field under the GenFlow (5) scheme does not decrease as rapidly as for GD. As a result, GenFlow can evade saddle points quickly. Specifically, we show that the time required to escape a neighborhood of the saddle point can be upper bounded by a constant independent of the size of the neighborhood. We impose the following assumption for the analysis in this section.

Assumption 1. *The objective function f belongs to the class C^2 .*

For functions satisfying the above assumption, a non-degenerate saddle point x^* is a point such that $\nabla f(x^*) = 0$ and $D^2 f(x^*)$ is non-singular. A non-degenerate saddle point also has the property that there exists $\lambda \in \sigma(D^2(f(x^*)))$ such that $\lambda < 0$. Saddle points that satisfy these properties are referred to in the literature [30], [37] as strict (or rideable) saddle points. Non-degenerate saddle points also have a useful property that local improvements are always possible in their neighborhood.

Theorem 3 below provides an upper bound on the length of the path under the GenFlow scheme in a neighborhood of a non-degenerate saddle point of the function f . The analysis is inspired by similar techniques in [20], and relies on the following key lemmas.

Lemma 3. *Assume that function f satisfies Assumption 1 and let x^* denote its non-degenerate saddle point. Let $H := D^2(f(x^*))$. Define $\tilde{d}(x) := \sqrt{(x - x^*)^T H (x - x^*)}$ for $x \in \mathbb{R}^n$, where $|B| := \sqrt{B^T B}$ for some square matrix B . Denote $\Lambda_{\max} := |\lambda|_{\max}(D^2 f(x^*))$ and $\Lambda_{\min} := |\lambda|_{\min}(D^2 f(x^*))$. Then for $a \geq 0$ the following relationships hold:*

$$\|x - x^*\| \leq \frac{a}{\sqrt{\Lambda_{\max}}} \implies \tilde{d}(x) \leq a, \quad (11)$$

$$\tilde{d}(x) \leq a \implies \|x - x^*\| \leq \frac{a}{\sqrt{\Lambda_{\min}}}. \quad (12)$$

Proof. The detailed proof is included in Appendix A. \square

In \mathbb{R}^n , the notion of distance is usually defined using the Euclidean norm. On the other hand, Lemma 3 introduces an alternative notion of distance $\tilde{d}(x)$, which is used later to prove Theorem 3. We also discuss on the relationship between the Euclidean distance and the alternative distance $\tilde{d}(x)$. The following lemma uses the Taylor theorem to derive a few useful local approximations.

Lemma 4. *Suppose the function f satisfies the Assumption 1 and has a non-degenerate saddle point x^* . Then for $k_1 > 0.5$, $k_2 < 1$ the following inequalities hold for some neighbourhood of x^**

$$|f(x) - f(x^*)| \leq k_1 \tilde{d}(x)^2 \quad (13)$$

$$\|\nabla f(x)\|_1 \geq k_2 \|H(x - x^*)\|_1. \quad (14)$$

Proof. The detailed proof is included in Appendix B. \square

Theorem 3. Suppose the function f satisfies the Assumption 1. Let x^* denote a non-degenerate saddle point of f . Let $x(t)$ be the solution of (5) with initial condition x_0 such that the solution $x(t)$ does not converge to the saddle point x^* . Then for all sufficiently small $r > 0$, the time spent in $B_r(x^*) \setminus \{x^*\}$ is bounded in the following way

$$\begin{aligned} \mathcal{L}^1(\{t \geq 0 : x(t) \in B_r(x^*) \setminus \{x^*\}\}) &\leq \\ \min \left\{ n^{\frac{1}{p-1}} \frac{8k_1}{k_2^{\frac{p}{p-1}}} \frac{\Lambda_{\max}^{\frac{p-2}{2(p-1)}}}{\Lambda_{\min}^{\frac{p}{2(p-1)}}} r^{\frac{p-2}{p-1}}, n^{\frac{1}{q-1}} \frac{8k_1}{k_2^{\frac{q}{q-1}}} \frac{\Lambda_{\max}^{\frac{q-2}{2(q-1)}}}{\Lambda_{\min}^{\frac{q}{2(q-1)}}} r^{\frac{q-2}{q-1}} \right\}, \end{aligned} \quad (15)$$

where $k_1 > 0.5$, $k_2 < 1$, $\Lambda_{\max} = |\lambda|_{\max}(D^2 f(x^*))$ and $\Lambda_{\min} = |\lambda|_{\min}(D^2 f(x^*))$.

Proof. The detailed proof is included in Appendix C. \square

Note that in equation (15) the exponent of the term $r^{\frac{p-2}{p-1}}$ is positive whereas the exponent of the term $r^{\frac{q-2}{q-1}}$ is negative. Hence as the radius r of the neighbourhood $B_r(x^*)$ increases the term $r^{\frac{p-2}{p-1}}$ increases whereas the term $r^{\frac{q-2}{q-1}}$ decreases. Thus at some finite value both the terms must be the same. Let the constant \hat{r} be such that

$$n^{\frac{1}{p-1}} \frac{8k_1}{k_2^{\frac{p}{p-1}}} \frac{\Lambda_{\max}^{\frac{p-2}{2(p-1)}}}{\Lambda_{\min}^{\frac{p}{2(p-1)}}} \hat{r}^{\frac{p-2}{p-1}} = n^{\frac{1}{q-1}} \frac{8k_1}{k_2^{\frac{q}{q-1}}} \frac{\Lambda_{\max}^{\frac{q-2}{2(q-1)}}}{\Lambda_{\min}^{\frac{q}{2(q-1)}}} \hat{r}^{\frac{q-2}{q-1}}. \quad (16)$$

Then for radius r satisfying the conditions of Theorem 3 it can be said that

$$\begin{aligned} \mathcal{L}^1(\{t \geq 0 : x(t) \in B_r(x^*) \setminus \{x^*\}\}) &\leq \\ n^{\frac{1}{p-1}} \frac{8k_1}{k_2^{\frac{p}{p-1}}} \frac{\Lambda_{\max}^{\frac{p-2}{2(p-1)}}}{\Lambda_{\min}^{\frac{p}{2(p-1)}}} \hat{r}^{\frac{p-2}{p-1}} &= n^{\frac{1}{q-1}} \frac{8k_1}{k_2^{\frac{q}{q-1}}} \frac{\Lambda_{\max}^{\frac{q-2}{2(q-1)}}}{\Lambda_{\min}^{\frac{q}{2(q-1)}}} \hat{r}^{\frac{q-2}{q-1}}, \end{aligned}$$

where \hat{r} satisfies (16). Note that the time required to escape the neighbourhood $B_r(x^*)$ is upper bounded by a constant that is independent of the size of the neighbourhood r .

Remark 3. Note that the above result holds true for initial conditions for which the trajectory does not converge to the saddle point. This is indeed true in most scenarios (see example in [28]).

IV. ACCELERATED FLOWS FOR MINIMAX PROBLEMS

The GenFlow scheme can further be extended to obtain solutions of strongly convex-strongly concave minimax problem:

$$\min_{x \in \mathbb{R}^{n_1}} \max_{y \in \mathbb{R}^{n_2}} g(x, y). \quad (17)$$

The function $g(\cdot, \cdot)$ is strongly convex-strongly concave with modulii μ_1, μ_2 if it is strongly convex in its first argument with modulus μ_1 and strongly concave in the second argument with modulus μ_2 . We consider the following saddle point dynamics:

$$\begin{aligned} \dot{x}_i &= -\frac{\nabla_{x_i} g(x, y)}{\|\nabla G\|_{p-1}^{\frac{p-2}{p-1}}} - \frac{\nabla_{x_i} g(x, y)}{\|\nabla G\|_{q-1}^{\frac{q-2}{q-1}}}, & \text{for } i = 1, 2, \dots, n_1, \\ \dot{y}_j &= \frac{\nabla_{y_j} g(x, y)}{\|\nabla G\|_{p-1}^{\frac{p-2}{p-1}}} + \frac{\nabla_{y_j} g(x, y)}{\|\nabla G\|_{q-1}^{\frac{q-2}{q-1}}}, & \text{for } j = 1, 2, \dots, n_2, \end{aligned} \quad (18)$$

with $p > 2$, $q \in (1, 2)$, and $\nabla G := [\nabla_x g^\top \quad -\nabla_y g^\top]^\top$. Note that the x and y dynamics in (18) are coupled through the norm of the total gradient vector ∇G . Along with the normalization, this coupling is also crucial for imparting fixed-time convergence as shown in the Theorem below:

Theorem 4 (Saddle point dynamics). Suppose the function $g : \mathbb{R}^{n_1} \times \mathbb{R}^{n_2} \rightarrow \mathbb{R}$ in (17) is strongly convex-strongly concave with modulii μ_1 and μ_2 , respectively. Then the saddle-point dynamics described in (18) converges to the unique optimal solution uniformly in a fixed amount of time, independent of the initialization.

Proof. Note that the saddle point is also characterized by the first-order stationarity condition, and since the function g is strongly convex-strongly concave in its arguments, the stationary point is indeed the saddle point (or the equilibrium of the saddle point dynamics (18)). The strong convexity-strong concavity translates to following set of conditions on the second-order partial derivatives:

$$\nabla_{xx}^2 g(x, y) \succcurlyeq \mu_1 I_{n_1} \quad \text{and} \quad \nabla_{yy}^2 g(x, y) \preccurlyeq -\mu_2 I_{n_2}. \quad (19)$$

In light of the stationarity conditions and the strongly convex-strongly concave assumptions, a natural choice for the candidate Lyapunov function is:

$$V := \frac{1}{2} \|\nabla_x g(x, y)\|^2 + \frac{1}{2} \|\nabla_y g(x, y)\|^2. \quad (20)$$

Taking time-derivative of V along the trajectories of (18) yields:

$$\begin{aligned} \dot{V} &= \nabla_x g(x, y)^\top \nabla_{xx}^2 g(x, y) \dot{x} + \nabla_y g(x, y)^\top \nabla_{yy}^2 g(x, y) \dot{y} \\ &\quad + \underbrace{(\nabla_x g(x, y)^\top \nabla_{xy}^2 g(x, y) \dot{y} + \nabla_y g(x, y)^\top \nabla_{xy}^2 g(x, y) \dot{x})}_{=0}, \end{aligned} \quad (21)$$

where the last term evaluates to zero following the saddle point dynamics. Substituting (18) into (21) results in:

$$\begin{aligned} \dot{V} &= (-\nabla_x g^\top \nabla_{xx}^2 g \nabla_x g + \nabla_y g^\top \nabla_{yy}^2 g \nabla_y g) \left(\frac{1}{\|\nabla G\|_{p-1}^{\frac{p-2}{p-1}}} \right. \\ &\quad \left. + \frac{1}{\|\nabla G\|_{q-1}^{\frac{q-2}{q-1}}} \right) \\ &\leq -\mu_1 \frac{\|\nabla_x g(x, y)\|^2}{\|\nabla G\|_{p-1}^{\frac{p-2}{p-1}} + \|\nabla G\|_{q-1}^{\frac{q-2}{q-1}}} - \mu_2 \frac{\|\nabla_y g(x, y)\|^2}{\|\nabla G\|_{p-1}^{\frac{p-2}{p-1}} + \|\nabla G\|_{q-1}^{\frac{q-2}{q-1}}}, \end{aligned} \quad (22)$$

where the last inequality follows from (19). Recall that $\|\nabla G\|^2 = \|\nabla_x g(x, y)\|^2 + \|\nabla_y g(x, y)\|^2$, resulting in:

$$\begin{aligned} \dot{V} &\leq -\min(\mu_1, \mu_2) \left(\|\nabla G\|^{2 \cdot \frac{p}{2(p-1)}} + \|\nabla G\|^{2 \cdot \frac{q}{2(q-1)}} \right) \\ &\leq -\min(\mu_1, \mu_2) \left((2V)^{\frac{p}{2(p-1)}} + (2V)^{\frac{q}{2(q-1)}} \right), \end{aligned} \quad (23)$$

which satisfies the sufficient condition for fixed-time convergence. \square

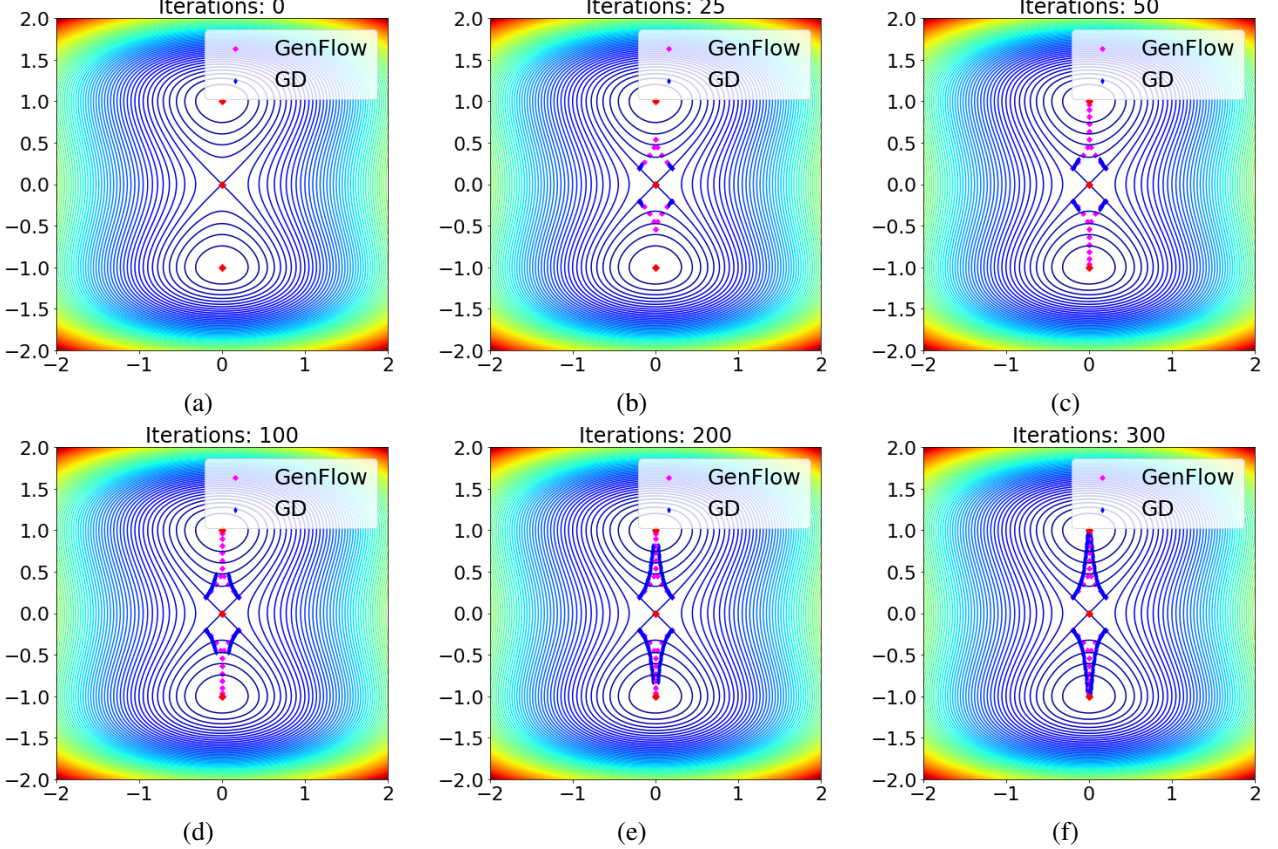


Fig. 1. Snapshots at different iterations for evasion of saddle points. GenFlow is able to evade the saddle points and converge to optimum in less than 50 iterations, while gradient descent requires more than 300 iterations for convergence.

V. EXPERIMENTS

Having analyzed the theoretically superior convergence behavior of GenFlow and its momentum variant, we now focus our attention to empirical performance of discretized-GenFlow scheme for a variety of tasks, involving (i) Accelerated evasion of non-degenerate saddle points, (ii) Training of deep neural networks for classification tasks, (iii) Training stabilization of generative adversarial networks (GANs) [32]. The GenFlow and its momentum variant were implemented using PyTorch’s inbuilt optimizer class, and can thus be easily integrated with any neural network training task. While GenFlow(M) is discretized as discussed in Remark 2, we use a simple forward-Euler discretization for GenFlow. Using similar techniques in [38][Theorem 2], it can be shown that under assumptions of strong-convexity or PL-inequality, the forward-Euler discretization results in (T, ϵ) -close discrete-time approximations of GenFlow and GenFlow(M), however, its detailed analysis is beyond the scope of the current study and left as part of the future work.

Fast Evasion of Non-Degenerate Saddle Points To illustrate fast evasion of saddle points, we consider the test function, $f(x, y) = 0.5x^2 + 0.25y^4 - 0.5y^2$, described in [28]. The function admits three isolated critical points: $z_1 = (0, 0)$, $z_2 = (0, -1)$, $z_3 = (0, 1)$, with z_1 being a non-degenerate saddle point, while z_2 and z_3 are isolated local minima. It is well known that the vanilla gradient descent may take exponential time to evade non-degenerate saddle points [29]. We, thus, benchmark GenFlow against the gradient descent for saddle

point evasion of the aforementioned test function. It can be seen in Figure 1 that while both gradient descent and GenFlow successfully escape the saddle point z_1 , the time of evasion is much smaller for GenFlow, as opposed to the gradient descent.

Datasets The accelerated convergence behavior of GenFlow for training of neural network classifiers is benchmarked on the two most widely datasets: MNIST (60k training images, 10k test images) [39]; and CIFAR10 (50k training images, 10k test images) [40]. Additionally, training stabilization of GANs is also benchmarked on the MNIST dataset.

Baseline optimizers We benchmark GenFlow(M) against the most widely used optimizers belonging to different families of first-order optimization algorithms: (i) RMSprop [41], (ii) Stochastic Variance Reduced Gradient (SVRG) [42], (iii) Adam [23], and (iv) FxTS-GF(M) [13]. The hyperparameters for each algorithm are tuned for optimal performance. For instance, it was observed that a large learning rate for Adam or rmsprop significantly destabilizes the training, and hence a suitably tuned smaller learning rate was chosen for classification problems.

Evaluation details For the classification tasks, the optimization algorithms are evaluated on three criteria: (i) Training cross-entropy loss, (ii) Training accuracy, and (iii) Testing accuracy (for evaluating the quality of local minima in terms of generalization capability). For the task of GAN training, the optimization algorithms are evaluated on three criteria: (i) Accuracy of images generated by the Generator (calculated using a pre-trained model available at: github.com/

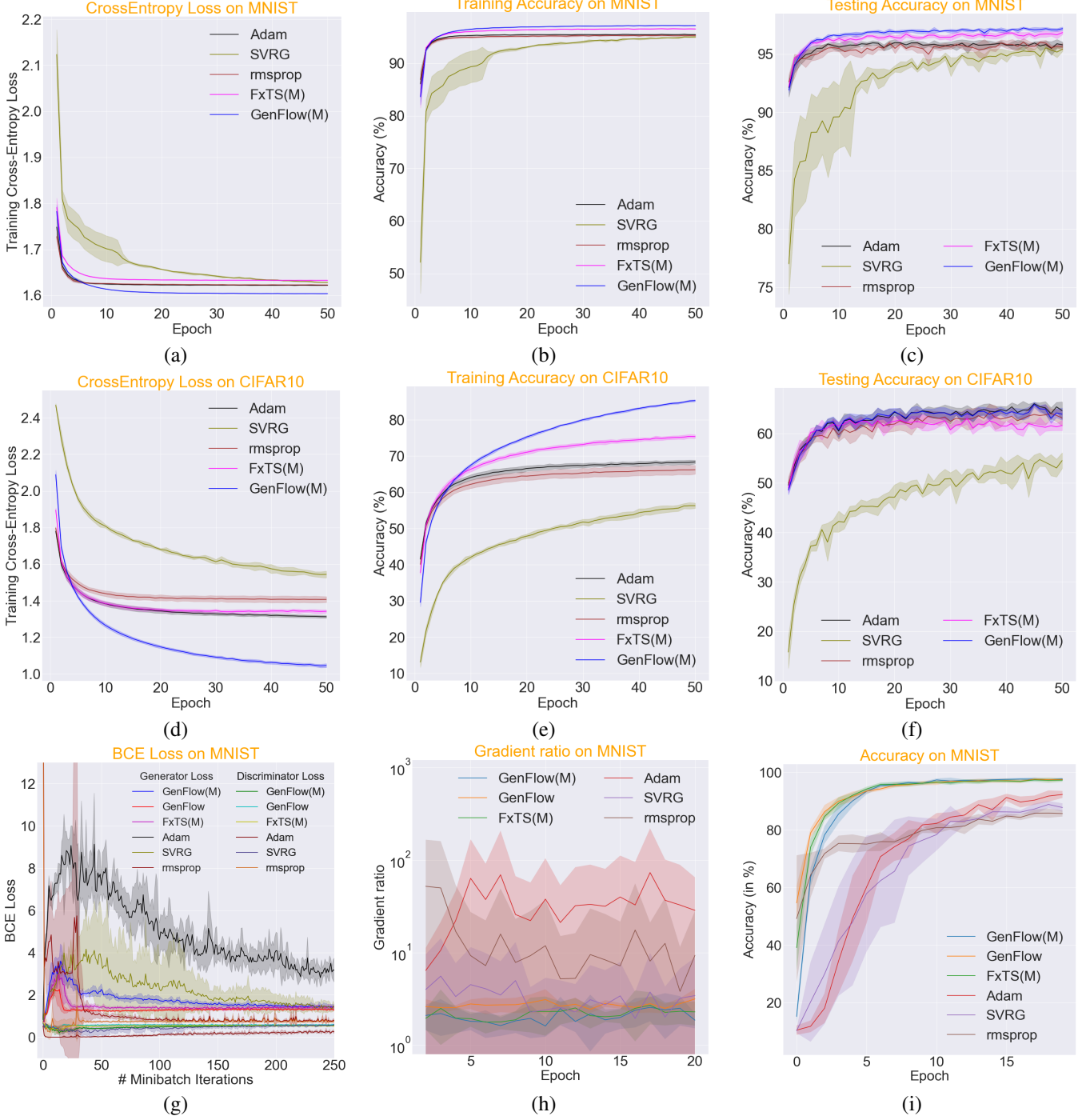


Fig. 2. Benchmarking GenFlow against SOTA optimizers for neural network based classification tasks and training stabilization of GANs: (a), (b), (c) indicate training and generalization performance of several optimizers on the MNIST dataset, while (d), (e), (f) analyze them on the CIFAR10 dataset. Items (g), (h), (i) depict training losses for GANs, gradient ratios for analyzing stabilization, and classification accuracy on images generated after each epoch, respectively.

aaron-xichen/pytorch-playground), (ii) Binary Cross Entropy (BCE) Loss of the Generator and the Discriminator, and (iii) Gradient Ratio, the ratio is equal to $\|grad_D^{(t)}\|_2/\|grad_D^{(0)}\|_2 + \|grad_G^{(t)}\|_2/\|grad_G^{(0)}\|_2$, where $grad_D^{(0)}$ (respectively $grad_G^{(0)}$) and $grad_D^{(t)}$ (respectively $grad_G^{(t)}$) are the initial and current gradients of Discriminator (respectively Generator) [43].

Network details For classification on the MNIST dataset, we have considered a network with a single convolutional

layer with ReLU activation (consisting of 32 filters of size 3×3), followed by a dense layer (with ReLU activation) of output size 128. The final linear layer transforms 128-dimensional input to a 10-dimensional output (corresponding to 10 classes) with SoftMax activation. Our architecture for CIFAR10 comprises of two convolutional layers, each followed by a max-pooling layer (with a 2×2 window). The convolutional layers comprise of 6 and 16 filters, each of size 5×5 with ReLU activation, respectively. This is followed by

two dense layers with ReLU activation (of sizes 120 and 84, respectively) and an output layer with SoftMax activation of size 10 (corresponding to 10 classes). We use ℓ_2 -regularized cross-entropy loss for the classification tasks. For experiments on training GANs, Conditional GAN (cGAN) with the following architecture is used: (i) Generator network consists of an input layer, two hidden layers and an output layer. Both the input and hidden layers comprise of 2D transposed batch normalized convolutional layer with ReLU activation, while the output layer is a simple 2D transposed convolutional layer with \tanh activation. The convolutional filter parameters, represented by the tuple (input dimension, output dimension, kernel size, stride), for the four layers in order are (74,256,3,2), (256,128,4,1), (128,64,3,2), and (64,1,4,2). (ii) Discriminator network is a simpler architecture comprising of input, hidden and output layers. Here, we use 2D transposed batch normalized convolutional layer with leaky ReLU activation (with 0.2 negative slope) for the input and the hidden layers. The output layer is a 2D convolutional layer without any nonlinear activation. The convolutional filter parameters for the three layers in order are (11,64,4,2), (64,128,4,2), and (128,1,4,2).

Training of Feedforward Neural Networks

For classification tasks on both MNIST and CIFAR10 datasets, we tune the hyperparameters for optimal performance. In particular, we arrived at the following optimizer settings for classification task on MNIST: (i) Adam ($\text{lr}=10^{-3}$), (ii) SVRG ($\text{lr}=10^{-2}$), (iii) RMSprop ($\text{lr}=10^{-3}$), (iv) FxTS(M) ($\text{lr}=10^{-2}$,momentum=0.7, $(p, q) = 20, 1.98$), (v) GenFlow(M) ($\text{lr}=10^{-2}$,momentum=0.9, $(p, q) = 10, 1.98$). Figure 2a represents the training cross-entropy loss as a function of epochs, while Figures 2b and 2c depict the corresponding training and test accuracies obtained using the aforementioned optimizers, and averaged across five random seeds. It can be seen that GenFlow(M) not only arrives at an optimal solution faster than other methods, the variance across the random seeds is significantly small. Both Adam and RMSprop could not be trained efficiently with higher learning rates, and the learning rates had to be reduced to 10^{-3} for optimal performance.

A similar behavior is observed on the CIFAR10 dataset (Figures 2d-f). While the generalization performance of these optimizers on test dataset is largely very similar (barring the SVRG method), the performance on the training dataset in terms of ℓ_2 -regularized cross-entropy loss, as well as training accuracy, is far better for the proposed GenFlow(M). The optimal performances were obtained using following hyperparameters: (i) Adam ($\text{lr}=10^{-3}$), (ii) SVRG ($\text{lr}=10^{-3}$), (iii) RMSprop ($\text{lr}=10^{-3}$), (iv) FxTS(M) ($\text{lr}=5 \times 10^{-3}$,momentum=0.7, $(p, q) = 20, 1.98$), (v) GenFlow(M) ($\text{lr}=5 \times 10^{-3}$,momentum=0.5, $(p, q) = 10, 1.98$). Here, lr represents the learning rate of an optimization algorithm.

Training of GANs

GenFlow(M) and GenFlow are further evaluated by training GANs on MNIST dataset. The performance of GenFlow(M) and GenFlow is benchmarked against the FxTS-GF(M), Adam, SVRG and RMSprop optimizers. For each optimizer, best hyperparameters are selected based on Accuracy of images generated by the Generator for 20 epochs, averaged over 3 seeds. After finding the best hyperparameters, the plots in

Figure 2g-i are obtained for 5 seeds. The values of best hyperparameter tuple (generator step size (lr), discriminator to generator step size ratio, momentum (if applicable)) for GenFlow, GenFlow(M), FxTS-GF(M), Adam, SVRG and RMSprop are (0.01, 5, $p = 2.1, q = 1.9, \beta_1 = 0.9, \beta_2 = 1.8$), (0.005, 5, 0.3, $p = 2.1, q = 1.9$), (0.01, 5, 0.2, $p = 2.1, q = 1.9$), (0.0002, 10), (0.05, 5), and (0.005, 5, 0.5) respectively. From the Figure 2i we can see that GenFlow(M) and GenFlow outperforms other methods by achieving optimal solution faster and having low variance across seeds. Figure 2h shows that GenFlow(M) and GenFlow has better training stability compared to other methods as the gradient ratio approximately stays near 1 [43]. Other details: (i) Mini-batch size = 128, (ii) Generator gaussian noise dimension = 64 (iii) GenFlow hyperparameters β_1 and β_2 are multiplied with 1st and 2nd term in RHS of (5) respectively. Images generated by the generator of each of the optimizers after 20 epochs are shown in Figure 3. From the figure, it can be seen that the Images generated by GenFlow(M) and GenFlow are qualitatively superior than the ones generated by the Adam, RMSprop and SVRG optimizers. The difference is clearly visible when we compare digits, such as 4, 5, 6, and 7.

VI. CONCLUSION

In this work, we propose the *GenFlow* gradient-flow scheme and its momentum variant which were shown to converge to the optimum of cost functions satisfying PL-inequality in fixed-time (i.e., the convergence time is finite and uniformly upper bounded irrespective of initial candidate solution). We further bound escape time from non-degenerate saddle points and show fixed-time convergence to the solution of minimax problems under suitable assumptions. Experimental results show superior convergence properties compared to state-of-the-art optimizers in training neural networks and GANs.

APPENDIX A PROOF OF LEMMA 3

Proof. The matrix H is a symmetric matrix. Thus its eigenvalue decomposition is given by $H = SDS^T$ where S is an orthogonal matrix and D is a diagonal matrix of the eigenvalues of H . Clearly $|D| = \sqrt{D^T D}$ is a diagonal matrix with modulus of the eigenvalues $\lambda \in \sigma(H)$ at the diagonal. Observe that $H^T H = SD^2 S^T$ and it can be easily proved that $|H| = \sqrt{H^T H} = S|D|S^T$. Now

$$\begin{aligned} \tilde{d}(x) &= \sqrt{(x - x^*)^T |H|(x - x^*)} \\ &= \sqrt{(x - x^*)^T S|D|S^T(x - x^*)} \\ &\leq \sqrt{(x - x^*)^T S \Lambda_{\max} I_d S^T(x - x^*)} \\ &= \sqrt{(x - x^*)^T \Lambda_{\max}(x - x^*)} \\ &= \sqrt{\Lambda_{\max}} \|x - x^*\|, \end{aligned} \tag{24}$$

where to prove the inequality the following fact has been used $\Lambda_{\max} I_n - |D| \succeq 0$. Thus, when $\|x - x^*\| \leq \frac{a}{\sqrt{\Lambda_{\max}}}$, then (11) holds.

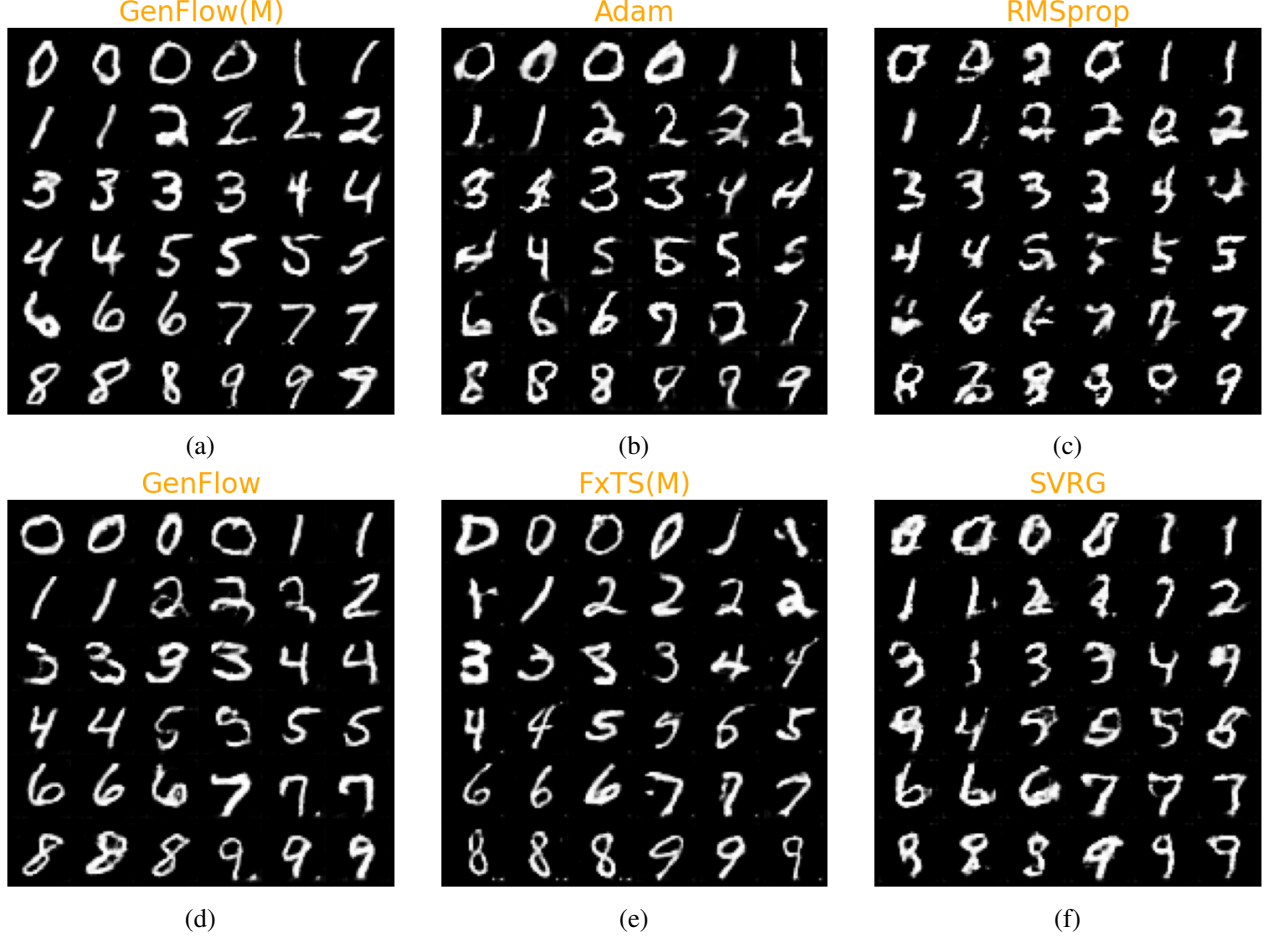


Fig. 3. Comparison of generator generated images after 20 epochs trained using different optimizers.

Similarly we obtain

$$\begin{aligned}\tilde{d}(x) &\geq \sqrt{(x - x^*)^T S \Lambda_{\min} I_d S^T (x - x^*)} \\ &= \sqrt{\Lambda_{\min}} \|x - x^*\|,\end{aligned}\quad (25)$$

where the inequality is proved using $|D| - \Lambda_{\min} I_n \succeq 0$. If $\tilde{d}(x) \leq a$ then by (25) we obtain $\sqrt{\Lambda_{\min}} \|x - x^*\| \leq a$, i.e., (12) is established. This concludes the proof. \square

APPENDIX B PROOF OF LEMMA 4

Proof. For the function f apply the Taylor's theorem at x^* to obtain

$$\begin{aligned}f(x) &= f(x^*) + \nabla f(x^*)^T (x - x^*) \\ &\quad + \frac{1}{2} (x - x^*)^T D^2(f(x^*)) (x - x^*) + R_2(x),\end{aligned}$$

where $R_2(x) \rightarrow 0$ as $\|x - x^*\| \rightarrow 0$. Using the fact $\nabla f(x^*) = 0$, we obtain

$$\begin{aligned}|f(x) - f(x^*)| &= \left| \frac{1}{2} (x - x^*)^T D^2(f(x^*)) (x - x^*) + R_2(x) \right| \\ &\leq \frac{1}{2} |(x - x^*)^T D^2(f(x^*)) (x - x^*)| + |R_2(x)| \\ &\leq \frac{1}{2} |(x - x^*)^T |H| (x - x^*)| + |R_2(x)| \\ &= \frac{1}{2} \tilde{d}(x)^2 + |R_2(x)|,\end{aligned}$$

where to obtain the second inequality the relation $|H| - H \succeq 0$ is used. As $\lim_{\|x - x^*\| \rightarrow 0} R_2(x) = 0$, for some neighbourhood of x^* and for $k_1 > 0.5$ it is true that $k_1 \tilde{d}(x)^2 \geq \frac{1}{2} \tilde{d}(x)^2 + |R_2(x)|$. Thus the inequality (13) is proved.

We now the Taylor's theorem for $\nabla f(x)$ at x^* to obtain

$$\begin{aligned}\nabla f(x) &= \nabla f(x^*) + D^2(f(x^*)) (x - x^*) + R_1(x) \\ &= H(x - x^*) + R_1(x),\end{aligned}$$

where the remainder term $R_1(x)$ satisfies $\lim_{\|x - x^*\|_1 \rightarrow 0} \|R_1(x)\|_1 = 0$. Taking the ℓ_1 norm on both the sides

$$\begin{aligned}\|\nabla f(x)\|_1 &= \|H(x - x^*) + R_1(x)\|_1 \\ &\geq \|H(x - x^*)\|_1 - \|R_1(x)\|_1.\end{aligned}$$

Now, for some $k_2 < 1$ it can be proved that $\|H(x - x^*)\|_1 - \|R_1(x)\|_1 \geq k_2\|H(x - x^*)\|_1$ holds for some neighbourhood of x^* which leads to (14) and concludes the proof. \square

APPENDIX C PROOF OF THEOREM 3

Proof. Without loss of generality, assume $x^* = 0$ and let $H := D^2(f(0))$. For $x \in \mathbb{R}^n$ define $\tilde{d}(x) := \sqrt{x^T H x}$, where $|B| := \sqrt{B^T B}$ for a square matrix B . Since the assumptions of Lemma 3-4 are satisfied their results can be used here. This also means that for some neighbourhood of $0 \in \mathbb{R}^n$ the relations (13) and (14) hold true. Now

$$\begin{aligned} \|\nabla f(x(t))\|_1 &\geq k_2\|Hx(t)\|_1 \geq k_2\|Hx(t)\|_2 \\ &= k_2\|H^{\frac{1}{2}}|H|^{\frac{1}{2}}x(t)\|_2 \\ &\geq k_2\sqrt{\Lambda_{\min}}\|H^{\frac{1}{2}}x(t)\|_2 = k_2\sqrt{\Lambda_{\min}}\tilde{d}(x(t)). \end{aligned} \quad (26)$$

To derive the second inequality above, the fact $\|v\|_1 \geq \|v\|_2$ for $v \in \mathbb{R}^n$ is used.

Using the chain rule, we obtain

$$\begin{aligned} \frac{d}{dt}f(x(t)) &= \sum_{i=1}^d \left(-|\nabla_i f(x(t))|^{\frac{p}{p-1}} - |\nabla_i f(x(t))|^{\frac{q}{q-1}} \right) \\ &= -\|\nabla f(x(t))\|^{\frac{p}{p-1}} - \|\nabla f(x(t))\|^{\frac{q}{q-1}} \\ &\leq -d^{\frac{-1}{p-1}}\|\nabla f(x(t))\|_1^{\frac{p}{p-1}} - d^{\frac{-1}{q-1}}\|\nabla f(x(t))\|_1^{\frac{q}{q-1}}, \end{aligned}$$

where to derive the inequality the relation $\|v\|_r \leq n^{\frac{1}{r} - \frac{1}{s}}\|v\|_s$ for $v \in \mathbb{R}^n$ and $s > r \geq 1$ has been used.

We now use the inequality (26) to obtain the following bound on the rate of change of $f(x(t))$:

$$\begin{aligned} -\frac{d}{dt}f(x(t)) &\geq \left(n^{\frac{-1}{p}}k_2\sqrt{\Lambda_{\min}}\right)^{\frac{p}{p-1}}\tilde{d}(x)^{\frac{p}{p-1}} \\ &\quad + \left(n^{\frac{-1}{q}}k_2\sqrt{\Lambda_{\min}}\right)^{\frac{q}{q-1}}\tilde{d}(x)^{\frac{q}{q-1}}. \end{aligned}$$

Let $k_3 = \left(n^{\frac{-1}{p}}k_2\sqrt{\Lambda_{\min}}\right)^{\frac{p}{p-1}}$ and $k_4 = \left(n^{\frac{-1}{q}}k_2\sqrt{\Lambda_{\min}}\right)^{\frac{q}{q-1}}$. Then one obtains

$$-\frac{d}{dt}f(x(t)) \geq k_3\tilde{d}(x)^{\frac{p}{p-1}} + k_4\tilde{d}(x)^{\frac{q}{q-1}}. \quad (27)$$

Let the approximations (13) and (26) be true inside the ball $B_{\hat{r}}(0)$ for $\hat{r} > 0$. Suppose that $x(t) \in B_{\hat{r}}(0)$ for $t \in [t_1, t_2]$. Let $e(t) := \tilde{d}(x(t))$ and now integrate (27) to get

$$f(x(t_1)) - f(x(t_2)) \geq k_3 \int_{t_1}^{t_2} e(s)^{\frac{p}{p-1}} ds + k_4 \int_{t_1}^{t_2} e(s)^{\frac{q}{q-1}} ds.$$

Let $r := \kappa^{-\frac{1}{2}}\hat{r}$ where $\kappa = \frac{\Lambda_{\max}}{\Lambda_{\min}}$. For $\eta \leq \sqrt{\Lambda_{\max}}r$ it is true that $\tilde{d}(x) \leq \eta$ implies $x \in B_{\hat{r}}(0)$. Let $t_0 > 0$ be the first time where $e(t) \leq \eta$ and t_3 be the last time when $e(t) \leq \eta$, i.e., $t_3 = \sup\{t \in [0, \infty] : e(t) \leq \eta\}$. The time t_3 is not assumed to be finite at this point but later it is proved that the length of the interval $[t_0, t_3]$ is bounded which in turn implies that t_3 is finite. If $t_3 = \infty$, then in an abuse of notation let $f(x(\infty)) = \lim_{t \rightarrow \infty} f(x(t))$, where note that the limit

exists since $f(x(t))$ is monotonically non-increasing by (27). Integrate over the interval $[t_0, t_3]$ to get the following

$$\begin{aligned} f(x(t_0)) - f(x(t_3)) &= \int_{t_0}^{t_3} -\frac{d}{ds}f(x(s))ds \\ &\geq \int_{e(s) \leq \eta} -\frac{d}{ds}f(x(s))ds \\ &\geq k_3 \int_{e(s) \leq \eta} e(s)^{\frac{p}{p-1}} ds \\ &\quad + k_4 \int_{e(s) \leq \eta} e(s)^{\frac{q}{q-1}} ds, \end{aligned}$$

where the fact $\frac{d}{dt}f(x(t)) \leq 0$ has been used to derive the first inequality and the second inequality has been derived using the inequality (27) over the intervals where $e(\cdot) \leq \eta$. Add and subtract $f(0)$ in the left hand side of the above inequality along with the bound (13) to get

$$2k_1\eta^2 \geq k_3 \int_{e(s) \leq \eta} e(s)^{\frac{p}{p-1}} ds + k_4 \int_{e(s) \leq \eta} e(s)^{\frac{q}{q-1}} ds.$$

As $e(\cdot) \geq 0$, the following two inequalities can be deduced

$$\int_{e(s) \leq \eta} e(s)^{\frac{p}{p-1}} ds \leq \frac{2k_1}{k_3}\eta^2 \quad (28)$$

$$\int_{e(s) \leq \eta} e(s)^{\frac{q}{q-1}} ds \leq \frac{2k_1}{k_4}\eta^2. \quad (29)$$

Using Markov's inequality [44], we obtain

$$\begin{aligned} \mathcal{L}^1 \left(\left\{ s : \frac{\eta^{\frac{p}{p-1}}}{2} \leq e(s)^{\frac{p}{p-1}} \leq \eta^{\frac{p}{p-1}} \right\} \right) \\ \leq \frac{2}{\eta^{\frac{p}{p-1}}} \int_{e(s)^{\frac{p}{p-1}} \leq \eta^{\frac{p}{p-1}}} e(s)^{\frac{p}{p-1}} ds \\ = \frac{2}{\eta^{\frac{p}{p-1}}} \int_{e(s) \leq \eta} e(s)^{\frac{p}{p-1}} ds \leq \frac{4k_1}{k_3}\eta^{\frac{p-2}{p-1}}, \end{aligned}$$

where to obtain the final inequality the relation (28) has been used. We now iteratively apply the Markov's inequality to obtain

$$\begin{aligned} \mathcal{L}^1 \left(\left\{ s : 0 < e(s)^{\frac{p}{p-1}} \leq \eta^{\frac{p}{p-1}} \right\} \right) \\ = \sum_{i=0}^{\infty} \mathcal{L}^1 \left(\left\{ s : \frac{\eta^{\frac{p}{p-1}}}{2^{i+1}} \leq e(s)^{\frac{p}{p-1}} \leq \frac{\eta^{\frac{p}{p-1}}}{2^i} \right\} \right) \\ \leq \sum_{i=0}^{\infty} \frac{4k_1}{k_3} \frac{\eta^{\frac{p-2}{p-1}}}{2^i} = \frac{8k_1}{k_3}\eta^{\frac{p-2}{p-1}}. \end{aligned}$$

Since $\{s : 0 < e(s) \leq \eta\} = \{s : 0 < e(s)^{\frac{p}{p-1}} \leq \eta^{\frac{p}{p-1}}\}$ one gets

$$\mathcal{L}^1(\{s : 0 < e(s) \leq \eta\}) \leq \frac{8k_1}{k_3}\eta^{\frac{p-2}{p-1}}. \quad (30)$$

Observe that $\{s : 0 < \|x(s)\| \leq r\} \subset \{s : 0 < \tilde{d}(x(s)) \leq \sqrt{\Lambda_{\max}}r\}$. Substituting $\eta = \sqrt{\Lambda_{\max}}r$ in (30), we obtain

$$\mathcal{L}^1(\{s : 0 < \|x(s)\| \leq r\}) \leq n^{\frac{1}{p-1}} \frac{8k_1}{k_2^{\frac{p}{p-1}}} \frac{\Lambda_{\max}^{\frac{p-2}{2(p-1)}}}{\Lambda_{\min}^{\frac{p}{2(p-1)}}} r^{\frac{p-2}{p-1}}. \quad (31)$$

Instead of using (28) one can use (29) and follow similar steps to obtain the following set of inequalities:

$$\begin{aligned}\mathcal{L}^1 \left(\{s : 0 < e(s)^{\frac{q}{q-1}} \leq \eta^{\frac{q}{q-1}}\} \right) &\leq \frac{8k_1}{k_4} \eta^{\frac{q}{q-1}}, \\ \mathcal{L}^1 \left(\{s : 0 < e(s) \leq \eta\} \right) &\leq \frac{8k_1}{k_4} \eta^{\frac{q-2}{q-1}}, \\ \mathcal{L}^1 \left(\{s : 0 < \|x(s)\| \leq r\} \right) &\leq n^{\frac{1}{q-1}} \frac{8k_1}{k_2^{\frac{q}{q-1}}} \frac{\Lambda_{\max}^{\frac{q-2}{2(q-1)}}}{\Lambda_{\min}^{\frac{q}{2(q-1)}}} r^{\frac{q-2}{q-1}}.\end{aligned}\quad (32)$$

Both (31) and (32) are upper bounds on the length of time spent in $B_r(x^*) \setminus \{x^*\}$ so it follows that both are satisfied if the smaller of the two bounds is satisfied. This concludes the proof. \square

REFERENCES

- [1] L. Bottou, F. E. Curtis, and J. Nocedal, “Optimization methods for large-scale machine learning,” *SIAM Review*, vol. 60, no. 2, pp. 223–311, 2018.
- [2] A. Beck, *First-order methods in optimization*. SIAM, 2017.
- [3] B. Polyak, “Some methods of speeding up the convergence of iteration methods,” *USSR Computational Mathematics and Mathematical Physics*, vol. 4, no. 5, pp. 1–17, 1964.
- [4] Y. Nesterov, “A method for unconstrained convex minimization problem with the rate of convergence $o(1/k^2)$,” vol. 269. Doklady AN SSR, 1983, pp. 543–547.
- [5] H. Li, C. Fang, and Z. Lin, “Accelerated first-order optimization algorithms for machine learning,” *Proceedings of the IEEE*, vol. 108, no. 11, pp. 2067–2082, 2020.
- [6] A. Wibisono, A. C. Wilson, and M. I. Jordan, “A variational perspective on accelerated methods in optimization,” *proceedings of the National Academy of Sciences*, vol. 113, no. 47, pp. E7351–E7358, 2016.
- [7] N. B. Kovachki and A. M. Stuart, “Continuous time analysis of momentum methods,” *Journal of Machine Learning Research*, vol. 22, no. 17, pp. 1–40, 2021.
- [8] H. Khalil, *Nonlinear Systems*. Prentice Hall, 2002.
- [9] L. Lessard, B. Recht, and A. Packard, “Analysis and design of optimization algorithms via integral quadratic constraints,” *SIAM Journal on Optimization*, vol. 26, no. 1, pp. 57–95, 2016.
- [10] P. Xu, T. Wang, and Q. Gu, “Accelerated stochastic mirror descent: From continuous-time dynamics to discrete-time algorithms,” in *International Conference on Artificial Intelligence and Statistics*. PMLR, 2018, pp. 1087–1096.
- [11] A. Orvieto and A. Lucchi, “Continuous-time models for stochastic optimization algorithms,” *Advances in Neural Information Processing Systems*, vol. 32, 2019.
- [12] O. Romero and M. Benosman, “Finite-time convergence in continuous-time optimization,” in *International Conference on Machine Learning*. PMLR, 2020, pp. 8200–8209.
- [13] P. Budhraja, M. Baranwal, K. Garg, and A. Hota, “Breaking the convergence barrier: Optimization via fixed-time convergent flows,” in *Proceedings of the AAAI Conference on Artificial Intelligence*, vol. 36, no. 6, 2022, pp. 6115–6122.
- [14] S. P. Bhat and D. S. Bernstein, “Finite-time stability of continuous autonomous systems,” *SIAM Journal on Control and Optimization*, vol. 38, no. 3, pp. 751–766, 2000.
- [15] J. Cortés, “Finite-time convergent gradient flows with applications to network consensus,” *Automatica*, vol. 42, no. 11, pp. 1993–2000, 2006.
- [16] A. Polyakov, “Nonlinear feedback design for fixed-time stabilization of linear control systems,” *IEEE Transactions on Automatic Control*, vol. 57, no. 8, pp. 2106–2110, 2011.
- [17] K. Garg and D. Panagou, “Fixed-time stable gradient flows: Applications to continuous-time optimization,” *IEEE Transactions on Automatic Control*, vol. 66, no. 5, pp. 2002–2015, 2021.
- [18] H. Karimi, J. Nutini, and M. Schmidt, “Linear convergence of gradient and proximal-gradient methods under the polyak-łojasiewicz condition,” in *Joint European Conference on Machine Learning and Knowledge Discovery in Databases*. Springer, 2016, pp. 795–811.
- [19] K. Y. Levy, “The power of normalization: Faster evasion of saddle points,” *arXiv preprint arXiv:1611.04831*, 2016.
- [20] R. Murray, B. Swenson, and S. Kar, “Revisiting normalized gradient descent: Fast evasion of saddle points,” *IEEE Transactions on Automatic Control*, vol. 64, no. 11, pp. 4818–4824, 2019.
- [21] A. C. Wilson, L. Mackey, and A. Wibisono, “Accelerating rescaled gradient descent: Fast optimization of smooth functions,” *Advances in Neural Information Processing Systems*, vol. 32, 2019.
- [22] L. Bottou, “Large-scale machine learning with stochastic gradient descent,” in *Proceedings of COMPSTAT’2010*. Springer, 2010, pp. 177–186.
- [23] D. P. Kingma and J. Ba, “Adam: A method for stochastic optimization,” *arXiv preprint arXiv:1412.6980*, 2014.
- [24] J. Duchi, E. Hazan, and Y. Singer, “Adaptive subgradient methods for online learning and stochastic optimization.” *Journal of Machine Learning Research*, vol. 12, no. 7, 2011.
- [25] S. Ruder, “An overview of gradient descent optimization algorithms,” *arXiv preprint arXiv:1609.04747*, 2016.
- [26] Y. Nesterov, *Introductory lectures on convex optimization: A basic course*. Springer Science & Business Media, 2003, vol. 87.
- [27] Y. N. Dauphin, R. Pascanu, C. Gulcehre, K. Cho, S. Ganguli, and Y. Bengio, “Identifying and attacking the saddle point problem in high-dimensional non-convex optimization,” *Advances in Neural Information Processing Systems*, vol. 27, 2014.
- [28] J. D. Lee, M. Simchowitz, M. I. Jordan, and B. Recht, “Gradient descent only converges to minimizers,” in *29th Annual Conference on Learning Theory*, ser. Proceedings of Machine Learning Research, vol. 49. PMLR, 2016, pp. 1246–1257.
- [29] S. S. Du, C. Jin, J. D. Lee, M. I. Jordan, B. Póczos, and A. Singh, “Gradient descent can take exponential time to escape saddle points,” in *Proceedings of the 31st International Conference on Neural Information Processing Systems*, ser. NIPS’17, 2017, p. 1067–1077.
- [30] R. Ge, F. Huang, C. Jin, and Y. Yuan, “Escaping from saddle points - online stochastic gradient for tensor decomposition,” in *Proceedings of The 28th Conference on Learning Theory, COLT 2015, Paris, France, July 3-6, 2015*, ser. JMLR Workshop and Conference Proceedings, vol. 40. JMLR.org, 2015, pp. 797–842.
- [31] D.-Z. Du and P. M. Pardalos, *Minimax and applications*. Springer Science & Business Media, 1995, vol. 4.
- [32] I. Goodfellow, J. Pouget-Abadie, M. Mirza, B. Xu, D. Warde-Farley, S. Ozair, A. Courville, and Y. Bengio, “Generative adversarial nets,” *Advances in Neural Information Processing Systems*, vol. 27, 2014.
- [33] A. Madry, A. Makelov, L. Schmidt, D. Tsipras, and A. Vladu, “Towards deep learning models resistant to adversarial attacks,” *arXiv preprint arXiv:1706.06083*, 2017.
- [34] J. O. Berger, *Statistical decision theory and Bayesian analysis*. Springer Science & Business Media, 2013.
- [35] Z. Zuo and L. Tie, “Distributed robust finite-time nonlinear consensus protocols for multi-agent systems,” *International Journal of Systems Science*, vol. 47, no. 6, pp. 1366–1375, 2016.
- [36] M. Muehlebach and M. I. Jordan, “Optimization with momentum: Dynamical, control-theoretic, and symplectic perspectives,” *Journal of Machine Learning Research*, vol. 22, no. 73, pp. 1–50, 2021.
- [37] J. Sun, Q. Qu, and J. Wright, “When are nonconvex problems not scary?” *arXiv preprint*, 2015.
- [38] K. Garg, M. Baranwal, R. Gupta, and M. Benosman, “Fixed-time stable proximal dynamical system for solving mvips,” *IEEE Transactions on Automatic Control*, pp. 1–8, 2022.
- [39] Y. LeCun, L. Bottou, Y. Bengio, and P. Haffner, “Gradient-based learning applied to document recognition,” *Proceedings of the IEEE*, vol. 86, no. 11, pp. 2278–2324, 1998.
- [40] A. Krizhevsky, “Learning multiple layers of features from tiny images,” *Technical Report, University of Toronto*, 2009.
- [41] G. Hinton, N. Srivastava, and K. Swersky, “Neural networks for machine learning lecture 6a overview of mini-batch gradient descent,” *Cited on*, vol. 14, no. 8, p. 2, 2012.
- [42] S. J. Reddi, A. Hefny, S. Sra, B. Poczos, and A. Smola, “Stochastic variance reduction for nonconvex optimization,” in *International conference on machine learning*. PMLR, 2016, pp. 314–323.
- [43] S. Jelassi, A. Mensch, G. Gidel, and Y. Li, “Adam is no better than normalized SGD: Dissecting how adaptivity improves GAN performance,” 2022. [Online]. Available: <https://openreview.net/forum?id=D9SuLzhgK9>
- [44] H. Federer, *Geometric Measure Theory*. Springer, 2014.